



D4.11.3: Documentation of aerosol typing products and tools



Deliverable number:	D4.11.3
Work package:	WP4 – Atmosphere
Intermediate Objective:	IO4.6
Deliverable type:	<input checked="" type="checkbox"/> Document, report
	<input type="checkbox"/> Websites, patent filings, videos, etc.
	<input type="checkbox"/> Other: please specify
Dissemination level:	<input checked="" type="checkbox"/> Public
	<input type="checkbox"/> Restricted
Estimated delivery (bimester):	B15
Actual delivery date:	DD/MM/YYYY
Author(s) (Partner-OU):	Nikolaos Papagiannopoulos, Pilar Gumà-Claramunt, Emilio Lapenna, Lucia Mona (CNR-IMAA),
Reviewed by:	Sara Basart (WMO), Angelika Dehn (ESA)
Note:	

IR0000032 – ITINERIS, Italian Integrated Environmental Research Infrastructures System - CUP B53C22002150006 (D.D. n. 130/2022)
 Funded by EU - Next Generation EU
 Mission 4 “Education and Research” - Component 2: “From research to business” -
 Investment 3.1: “Fund for the realization of an integrated system of research and innovation infrastructures”

Table of Contents

1.	<i>INTRODUCTION</i>	5
2.	<i>AEROSOL TYPING PRODUCTS</i>	5
2.1	Description of aerosol typing products	5
2.2	Product generation	9
2.3	Product availability	10
2.4	Results	11
3.	<i>AUXILIARY AEROSOL TYPING TOOLS</i>	13
4.	<i>DISCUSSION AND OUTLOOK</i>	14
	<i>REFERENCES</i>	15

Index of Tables and Figures

Table 1. Optical properties needed for the available lidar configurations (1-6) in HETEAC-Flex. β stands for the aerosol backscatter coefficient, α stands for the aerosol extinction coefficient, and the subscript corresponds to the wavelength for which the optical property refers to.....9

Figure 1:	Flowchart of the SCC and PPS products on-fly data flow.	10
Figure 2:	532-nm Attenuated backscatter coefficient (up) and 532-nm volume depolarization ratio (down) measured by the CIAO lidar POLPO during 28-30 April 2024.	11
Figure 3:	HiRAC aerosol classification retrieved by the CIAO lidar POLPO during 28-30 April 2024.	12
Figure 4:	MAC (up) and HETEAC-Flex (down) outputs superimposed on the 532-nm volume depolarization ratio time-height cross section retrieved by the CIAO lidar POLPO during 28 – 30 April 2024. The color-coded boxes correspond to different aerosol types.	12
Figure 5:	AERONET real (left) and imaginary (right) part of the refractive index for volcanic ash and desert dust.	13
Figure 6:	HiRAC aerosol classification retrieved by the CIAO lidar POLPO during 30-31 March 2024. The cyan lines indicate the AERONET measurements for which are given the aerosol type, the complex refractive index at 440 nm, and AOD at 440 nm.....	14

Index of Tables and Figures

<i>Abbreviation</i>	<i>Definition</i>
ABLH	Atmospheric boundary layer height
ACTRIS	Aerosol, Clouds, and Trace Gases Research Infrastructure
AERONET	Aerosol Robotic Network
AOD	Aerosol Optical Depth
API	Application Programming Interface
B	Bimester
CIAO	CNR-IMAA Atmospheric Observatory
CNR	Consiglio Nazionale delle Ricerche
CNS	Coarse-Nonspherical
CPU	Central Processing Unit
CR	Color Ratio
CS	Coarse
DOI	Digital Object Identifier
EARLINET	European Aerosol Research Lidar Network
EarthCARE	Earth Cloud, Aerosol and Radiation Explorer
ELDA	EARLINET Lidar Data Analyzer
ELIC	EARLINET Lidar Calibrator
ELPP	EARLINET Lidar Pre-Processor
EU	European Union
EWA	Early Warning for Aviation
FSA	Fine Spherical Absorbing aerosol
FSNA	Fine Spherical Non-Absorbing aerosol
GB	Giga byte
GUI	Graphical User Interface
HD	Hard Disk
HETEAC	Hybrid End-To-End Aerosol Classification
HETEAC-FLEX	Hybrid End-To-End Aerosol Classification-Flexible
HIRAC	High Resolution Aerosol Classification
HSRL,	High Spectral Resolution Lidar
IMAA	Istituto di Metodologie per l'Analisi Ambientale
ITINERIS	Italian Integrated Environmental Research Infrastructures System
MAC	Mahalanobis Aerosol Classification
NATALI	Neural network Aerosol Typing Algorithm based on Lidar data
NetCDF	Network Common Data Form
POLPO	Potenza Lidar for Particle Observations
PPS	Post Processing Server
RAM,	Random-access Memory
SCC	Single Calculus Chain
SQL	Structured Query Language
SYLVA	A System for Real Time Observation of Aeroallergens
TB	Tera Byte

1. INTRODUCTION

This document builds on the Deliverable: D4.11.1 “*Report on the organization of test cases for aerosol typing method improvements*”, where the aerosol typing methods and input data are outlined, and has a twofold goal. The first goal is to document the developed server infrastructure and associated results in close relation to Activity 4.11 and the Activities of WP4-Atmosphere altogether. The second is to present recent developments that could enhance the existing aerosol typing algorithms.

To date, several automatic aerosol typing schemes have been developed within ACTRIS/EARLINET and provide the predominant aerosol type or aerosol mixture in the atmosphere (Nicolae et al., 2018; Papagiannopoulos et al., 2018; Floutsi et al., 2024; del Águila et al., 2025). Since ITINERIS started, two of these typing algorithms got published highlighting the relevance of aerosol typing. Additionally, the launch of EarthCARE (<https://earth.esa.int/eogateway/missions/earthcare>) in 2024 calls for the validation of its aerosol classification scheme that plays an important role in radiative-closure assessments.

ITINERIS offers an opportunity to develop an infrastructure for an operational delivery of aerosol typing products taking profit of the ACTRIS/EARLINET database as well as the ACTRIS’s Single Calculus Chain (SCC; <https://docs.scc.ima.cnr.it/en/latest/introduction.html>). Thus, this Activity builds a server infrastructure that aims to output multiple aerosol classification products to serve research and community with this highly sought information.

This deliverable is organized as follows: Section 2 focuses on the aerosol classification products’ workflow as well as the data product description. Moreover, a brief discussion on the results of the available typing methods is presented. Section 3 briefly describes a new methodology for the separation of volcanic ash and desert dust that will improve the aerosol typing output. The document closes with Conclusions in Section 4.

2. AEROSOL TYPING PRODUCTS

The aerosol classification techniques can be separated in map and profile aerosol typing depending on the input parameters. **Map aerosol typing** refers to a 2D (time×height) output and uses, for the purposes of this document, calibrated lidar signals (i.e., SCC-ELIC products; see <https://docs.scc.ima.cnr.it/>). **Profile aerosol typing**, instead, refers to a 1D (height) output and uses aerosol optical properties (i.e., SCC-ELDA products). Currently, 3 aerosol typing products exist and will be described below:

- *Map aerosol typing: HiRAC,*
- *Profile aerosol typing: MAC, and HETEAC-Flex.*

2.1 Description of aerosol typing products

HiRAC

HiRAC (High Resolution Aerosol Classification) provides temporally high-resolution aerosol classification. The aerosol type product is separated into four aerosol classes (small, large spherical, mixture, large non-spherical) and can be retrieved independently of the light conditions as the methodology relies on elastic channels. The classification is based on aerosols’ physical features (shape and size) and not on the source origin.

The general methodology and the typing thresholds are described in Baars et al. (2017). Furthermore, a modification of the general methodology, which *HiRAC* is based upon, is presented in Papagiannopoulos et al. (2020).

Currently the **filename** of the *HiRAC* output is codified as follows:

Typing_AerRemSen_ccc_Levzz_HIRAC_YYYYMMDDHHMM_yyyymmddhhmm_vxx.nc

- **ccc** (length=3) reports a three-digit code representing univocally an ACTRIS/EARLINET station.
- **Levzz** (length=5) reports the level of the product. Levels are assigned to the product based on the specific quality control procedure (see <https://www.earlinet.org/index.php?id=293>). Currently only Lev01 is allowed to the typing product.
- **YYYYMMDDHHMM** (length=12) reports the start date and time of the measurements that the product file is linked with. The time is UTC.
- **yyymmddhhmm** (length=12) reports the stop date and time of the measurements that the product file is linked with. The time is UTC.
- **vxx** reports the version of the file. The character “v” is fixed. The next 2 characters are numeric (e.g., v01 means version 1 of the file, v02 version 2, etc.).

The following variables are included in the *HiRAC* data products:

- **aerosol_classification(time, altitude):** holds the aerosol classification. The values of the variable and the associated aerosol type in parentheses: 0.5 (Clean atmosphere), 1.5 (Not-typed), 2.5 (Aerosol: small), 3.5 (Aerosol: large-spherical), 4.5 (Aerosol: mixture, partly-nonspherical), 5.5 (Aerosol: large, nonspherical);
- **aerosol_backscatter_0532(time, altitude):** holds the 532 nm particle backscatter coefficient at that time and altitude. The high-resolution particle backscatter coefficient is retrieved following Papagiannopoulos et al. (2020) and requires the ELIC product;
- **aerosol_backscatter_1064(time, altitude):** holds the 1064 nm particle backscatter coefficient at that time and altitude. The high-resolution particle backscatter coefficient is retrieved following Papagiannopoulos et al. (2020) and requires the ELIC product;
- **aerosol_depolarization_0532(time, altitude):** holds the 532 nm particle depolarization ratio at that time and altitude;
- **longitude:** holds the longitude in degrees east of the ACTRIS/EARLINET station;
- **latitude:** holds the latitude in degrees north of the ACTRIS/EARLINET station.
- **station_altitude:** holds the station altitude above sea level of the ACTRIS/EARLINET station.
- **time:** holds the central time for which the optical property profile is reported. This is linked to the time dimension.
- **altitude:** holds the altitude for which the profiles are reported. The altitude grid is set up by the pre-processing module ELPP and it is reported above the sea level. This variable is linked to the altitude dimension.

MAC

The *MAC* (Mahalanobis Aerosol Classification) product provides an aerosol classification mask based on ACTRIS/EARLINET optical properties. The methodology is described in Papagiannopoulos et al. (2018).

Currently the **filename** of the *MAC* output is codified as follows:

Typing_AerRemSen_ccc_Levzz_MAC_YYYYMMDDHHMM_yyyymmddhhmm_vxx.nc

- **ccc** (length=3) reports a three-digit code representing univocally an ACTRIS/EARLINET station (see Section 3)

- **Levzz** (length=5) reports the level of the product. Levels are assigned to the product based on the specific quality control procedure (see <https://www.earlinet.org/index.php?id=293>). Currently only Lev01 is allowed to the typing products.
- **YYYYMMDDHHMM** (length=12) reports the start date and time of the measurements that the product file is linked with. The time is UTC.
- **yyyymmddhhmm** (length=12) reports the stop date and time of the measurements that the product file is linked with. The time is UTC.
- **vxx** reports the version of the file. The character “v” is fixed. The next 2 characters are numeric (e.g., v01 means version 1 of the file, v02 version 2, etc.).

The following variables specific for the *MAC* output are included (the common variables with *HiRAC* are not reported):

- **aerosol_classification(layers):**
holds the aerosol type related to different identified layers in the profile. The values of the variable and the associated aerosol type in parentheses: 0 (Not classified), 1 (clean continental), 2 (smoke), 3 (dust), 4 (marine), 5 (polluted dust), 6 (polluted continental), 7 (mixed dust);
- **angstrom_exponent(layers):**
holds the mean-layer backscatter-related Ångström exponent (532/1064);
- **lidar_ratio(layers):**
holds the mean-layer 532 nm lidar ratio;
- **ratio_of_lidar_ratios(layers):**
holds the mean-layer ratio of lidar ratios (355 nm and 532 nm);
- **depolarization(layers):**
holds the mean-layer 532 nm particle linear depolarization ratio.

HETEAC-Flex

HETEAC-Flex is a classification scheme based on EarthCARE’s HETEAC (Wandinger et al., 2023; Hybrid End-To-End Aerosol Classification), yet its methodological flexibility allows for the use of different lidar configurations. EarthCARE is equipped with a 355-nm HSRL, hence the typing relies on the use of 355-nm lidar ratio and 355-nm particle depolarization ratio. *HETEAC-Flex* builds on the same methodology and accommodates more complex lidar configurations with the most complex being a $3\beta+2\alpha+3\delta$ configuration. Consequently, *HETEAC-Flex* is an important tool in the assessment of EarthCARE’s aerosol classification by using ACTRIS/EARLINET ground-based lidars.

Currently the **filename** of the *HETEAC-Flex* output is codified as follows (the common variables with *HiRAC* and *MAC* are not reported):

Typing_AerRemSen_ccc_Levzz_HETEACFLEX_YYYYMMDDHHMM_yyyymmddhhmm_vxx.nc

- **ccc** (length=3) reports a three-digit code representing univocally an EARLINET station (see section3)
- **Levzz** (length=5) reports the level of the product. Levels are assigned to the product based on the specific quality control procedure (see <https://www.earlinet.org/index.php?id=293>). Currently only Lev01 is allowed to the typing product.
- **YYYYMMDDHHMM** (length=12) reports the start date and time of the measurements that the product file is linked with. The time is UTC.
- **yyyymmddhhmm** (length=12) reports the stop date and time of the measurements that the product file is linked with. The time is UTC.
- **vxx** reports the version of the file. The character “v” is fixed. The next 2 characters are numeric (e.g., v01 means version 1 of the file, v02 version 2, etc.).

The following variables specific for the *HETEAC_Flex* output are included (the common variables with *HiRAC* and *MAC* are not reported):

- **aerosol_type_initial_guess(layers):**
holds the aerosol type related to different identified layers in the profile. This variable corresponds to the initial guess of the state vector. The values of the variable and the associated aerosol type in parentheses: 1 (CS), 2 (FSA), 3 (FSNA), 4 (CNS), 5 (CNS/CS), 6 (CNS/FSA), 7 (CNS/FSNA), 8 (FSA/FSNA), 9 (FSNA/CS), 10 (Not-typed), nan (typing not possible);
- **aerosol_type_optimal_solution(layers):**
holds the aerosol type related to different identified layers in the profile. This variable corresponds to the optimal solution after convergence. The values of the variable and the associated aerosol type in parentheses: 1 (CS), 2 (FSA), 3 (FSNA), 4 (CNS), 5 (CNS/CS), 6 (CNS/FSA), 7 (CNS/FSNA), 8 (FSA/FSNA), 9 (FSNA/CS), 10 (Not-typed), nan (typing not possible);
- **aerosol_type_statistical_significance(layers):**
holds the aerosol type related to different identified layers in the profile. This variable corresponds to whether the optimal solution is statistically significant at 95%. The values of the variable and the associated aerosol type in parentheses: 1 (CS), 2 (FSA), 3 (FSNA), 4 (CNS), 5 (CNS/CS), 6 (CNS/FSA), 7 (CNS/FSNA), 8 (FSA/FSNA), 9 (FSNA/CS), 10 (Not-typed), nan (typing not possible);
- **CR(layers):**
holds the mean backscatter-related Color ratio (532/1064);
- **depol_355(layers):**
holds the mean 355-nm particle depolarization ratio;
- **depol_532(layers):**
holds the mean 532-nm particle depolarization ratio;
- **ext_Ang(layers):**
holds the mean extinction-related Angstrom exponent (355/532);
- **lr_355(layers):**
holds the mean 355-nm lidar ratio;
- **lr_532(layers):**
holds the mean 532-nm lidar ratio;
- **base(layers):**
holds the layer base of each of the layers identified. The layers were identified using the wavelet correlation transform method;
- **top(layers):**
holds the layer top of each of the layers identified. The layers were identified using the wavelet correlation transform method.

Users are strongly advised to use as first option the variable *aerosol_type_statistical_significance* and as second the *aerosol_type_optimal_solution* only to improve statistics. Furthermore, the number of the intensive properties in the *HETEAC_Flex* output depends on the input parameters. The list of the input configurations is given in Table 1:

Table 1. Optical properties needed for the available lidar configurations (1-6) in HETEAC-Flex. β stands for the aerosol backscatter coefficient, α stands for the aerosol extinction coefficient, and the subscript corresponds to the wavelength for which the optical property refers to.

Configuration	β_{355}	β_{532}	α_{355}	α_{532}	β_{1064}
1	×		×		
2		×		×	
3	×		×	×	
4		×		×	×
5	×	×	×	×	
6	×	×	×	×	×

The ramifications and related uncertainties of the presented typing algorithms are discussed in length in the publications that introduce the respective algorithms.

2.2 Product generation

The generation of the aerosol classification products is done in a dedicated server called Post-Processing Server (PPS). The scope of PPS is to provide additional products based on SCC products, originating either from the SCC or from the ACTRIS/EARLINET database.

PPS is hosted at CNR-IMAA and is built modularly, so that new products can be added as new modules and run independently. The server comprises 8 vCPU, 32GB RAM, and 100GB HD, with an additional data storage of 1 TB.

Before the full processing chain becomes operational, new products can be internally used and tested. Currently, besides the aerosol typing products, the server hosts a lidar pollen-specific product, an aerosol layer identification product, and a lidar-based early warning for aviation product.

Two possible setup configurations are designed:

- An **on-fly** procedure that generates the products right after they are generated by the SCC, using the SCC products as direct input.
- An **on-demand** procedure that generates the products for past periods, using as input the products that are available in the ACTRIS/EARLINET database.

The reason for the two separate configurations is to maintain full traceability of all the products involved in the production chain. For the *on-fly* procedure, the generated products are not stored permanently and can be overwritten and change if they are reprocessed, and therefore this process can only be applied to the data that is being currently processed. For the *on-demand* procedure, the aerosol typing products are generated for past data, and the plan is to use as input the data from the ACTRIS/EARLINET database, which is version controlled and therefore allows for the full traceability of the data used by the aerosol typing modules.

Currently, the setup of the *on-demand* procedure is ongoing, whilst the implementation of the *on-fly* procedure is planned for the second half of 2025.

The PPS has a dedicated postprocessing PostgreSQL database (version 16, running on a separate server with 6 vCPU, 16GB RAM, 60GB HD). Currently, it stores the outcome of the modules runs, which helps monitoring the input, output and possible errors generated. In the future, this database will also be used by the server for the product control generation (i.e., for a certain station and period, run the *HiRAC* module and upload it automatically to the ACTRIS/EARLINET database; for another station run the module without uploading, or for another station do not run the module at all).

In Figure 1, we present the current flowchart of the SCC and PPS products of the *on-fly* procedure. After the SCC products are generated, the postprocessing server runs the typing modules for the target measurements and stores the outputs in the data storage file system in the same server. Then, if the automatic upload is set up for those products, an upload application is triggered, which uploads the aerosol typing products into the ACTRIS/EARLINET database.

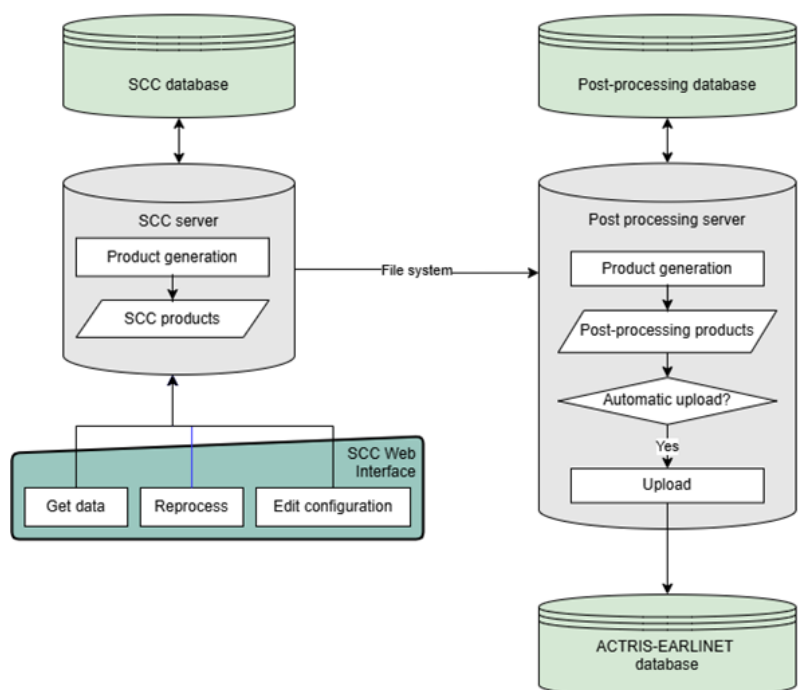


Figure 1: Flowchart of the SCC and PPS products on-fly data flow.

2.3 Product availability

Currently, the aerosol typing products are still in testing phase, and they can be shared on demand. After the initial phases of testing, the typing products available in the ACTRIS/EARLINET database will be made publicly available via the [data.earlinet.org API](https://data.earlinet.org), where the products' metadata will be shown and the products will be downloadable. At a later stage, they will also be available through the <https://data.earlinet.org/> web interface.

The focus so far has been given to the CIAO (CNR-IMAA Atmospheric Observatory) boundary layer campaign measurement (ABLH) campaign (for more details see D4.15.2) that took place at CNR-IMAA (40.60N, 15.72E, 760 m a.s.l.) from 15 April 2024 up to 1 May 2024. The campaign had the goal to use different types of remote sensing instruments operating simultaneously and continuously 24/7 together with frequent radiosondes' launches to establish a reference dataset for the ABLH retrieval. The related aerosol typing datasets will be soon openly available and associated with a DOI through the ITINERIS HUB.

The periodic run of the aerosol typing modules is set to once per day according to our operational plan. For now, the station of Potenza is considered and at a slow rate more lidar stations will be incorporated. The output shown in the following sub-section refer to the lidar station of Potenza.

2.4 Results

During the testing phase, we had the opportunity to assess the aerosol typing products taking profit of the *on-demand* procedure. For this, we used the CNR-IMAA measurement campaign related to the activities of Activity 4.15 and the abovementioned measurement campaign.

Here, we focus on a 3-day period (28–30 April 2024), when an important dust intrusion was observed over CNR-IMAA and captured by the lidar system POLPO (Potenza Lidar for Particle Observations). The lidar measurements indicate the presence of dust in the ABLH for the period examined and in a thicker layer residing over the ABLH from 18:00 UTC on 28 April until 18:00 UTC on 30 April. Figure 2 shows the calibrated attenuated backscatter at 532 nm (upper panel) and the calibrated volume depolarization ratio at 532 nm (lower panel) respectively. The white stripes either correspond to the required dark measurements needed for the transition from daytime to nighttime or to failures of the acquisition module.

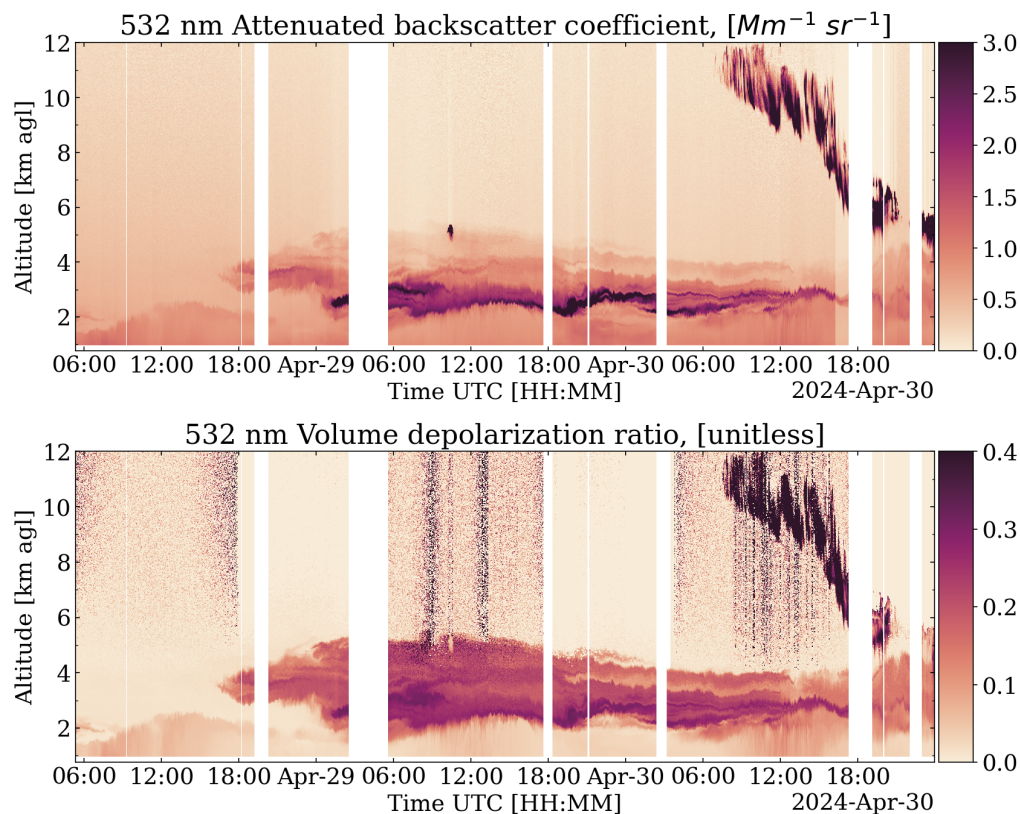


Figure 2: 532-nm Attenuated backscatter coefficient (up) and 532-nm volume depolarization ratio (down) measured by the CIAO lidar POLPO during 28-30 April 2024.

The *HiRAC* output in Figure 3 designates the presence of dust particles (black pixels; aerosol: large-nonspherical) for the whole timespan of the measurements, and particularly the aerosol layers above the ABLH. Also, mixed dust particles dominate the lower part of the atmosphere (scarlet pixels; aerosol: mixture, partly-nonspherical) while small aerosols (gold pixels; aerosol: small) indicative of pollution can also be seen in small segments of the figure in low lying layers. In comparison with Figure 2, the white stripes increased due to the failure of the typing module.

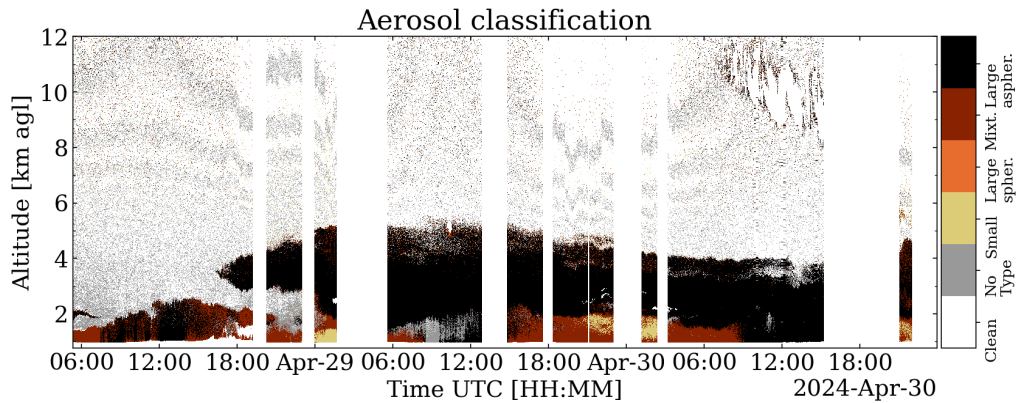


Figure 3: HiRAC aerosol classification retrieved by the CIAO lidar POLPO during 28-30 April 2024.

For the same aerosol scene, the *MAC* (upper panel) and *HETEAC-Flex* (lower panel) aerosol classifications are presented in Figure 4. The aerosol types of the algorithms were modified to correspond to the four aerosol categories of *HiRAC* to ease the interpretation of the plots. It is also worth noting that both *MAC* and *HETEAC-Flex* are available during nighttime operation in contrast to *HiRAC* that is available independently of the light conditions. In general terms, *MAC* and *HETEAC-Flex* mostly agree within the main dust feature arguably due to the strong dust signature on the depolarization ratio measurement. Differences exist in the first layers identified with *HETEAC-Flex* assigning these layers to the marine category. As a first guess for this behaviour, we hypothesize that is due to the low lidar ratio values indicative of the marine particles (e.g., Dawson et al 2015; Papagiannopoulos et al., 2018). Profile aerosol typing requires profiles of type-dependent intensive properties such as the lidar ratio to assign an aerosol type.

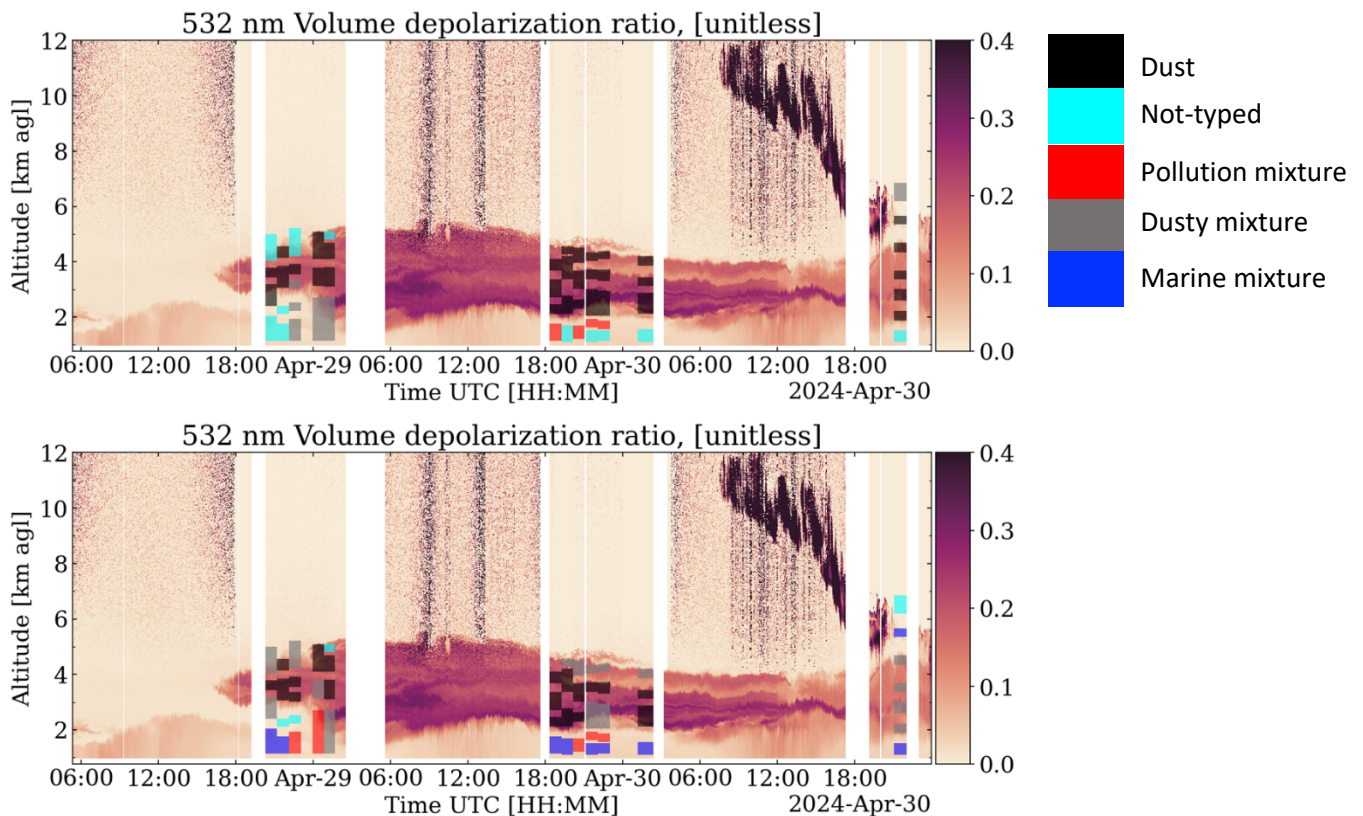


Figure 4: *MAC* (up) and *HETEAC-Flex* (down) outputs superimposed on the 532-nm volume depolarization ratio time-height cross section retrieved by the CIAO lidar POLPO during 28 – 30 April 2024. The color-coded boxes correspond to different aerosol types.

3. AUXILIARY AEROSOL TYPING TOOLS

A known issue for aerosol typing is the separation of volcanic ash and desert dust in lidar signals. Volcanic ash and desert dust are non-spherical, coarse-mode aerosols, and they tend to have high depolarization ratios with respect to other aerosol types. However, several studies document the differences, although slight, in particle depolarization ratio and lidar ratio (Ansmann et al., 2011; Gross et al., 2012). For instance, Papagiannopoulos et al. (2020) include these aerosol types in their automatic classification scheme (i.e., *MAC*) but they explicitly point out the difficulty to separate among volcanic ash and desert dust considering the variability in transport patterns, ageing, and type definition.

On the other hand, microphysical properties of volcanic ash and desert dust are shown to have significant differences. Airborne in situ measurements (e.g., Weinzierl et al., 2012) as well as photometer measurements (e.g., Mortier et al., 2013) highlight the differences in the complex refractive index with volcanic ash being more absorbing. This pattern can be seen in Figure 5 where the real and imaginary part of the refractive index for volcanic ash is greater than this of desert dust across the different wavelengths. The data are AERONET Level 2 and only comprise volcanic ash and desert dust. The volcanic ash dataset was specifically selected during the eruption of Eyjafjallajökull in 2010 for stations in north Europe. The desert dust dataset refers to measurements in Potenza in Italy. Both datasets were filtered following widely used filtering techniques. The main message from this plot is the importance of the imaginary part of the refractive index and at a lesser extent of the real part across the wavelength spectrum in separating ash and dust.

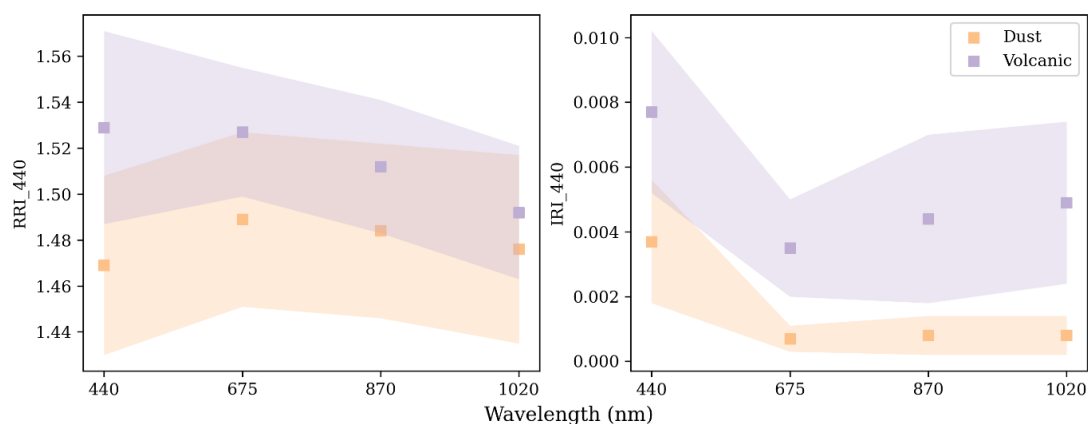


Figure 5: AERONET real (left) and imaginary (right) part of the refractive index for volcanic ash and desert dust.

We developed a methodology that synergistically uses lidar measurements and photometer microphysical retrievals. This approach comprises two steps. The first step uses photometer observations to build an aerosol model containing volcanic ash and desert. The second step includes two sub-steps which are the lidar depolarization measurements to identify the non-spherical particles and concurrent AERONET measurements to separate among ash and dust.

In the following, we applied the methodology on a dust event in Potenza on 30–31 March 2024. Figure 6 shows the *HiRAC* product and superimposed in cyan the AERONET almucantar measurements for the retrieval of the microphysical properties. The boxes contain the aerosol type, complex refractive index values, and AOD at 440 nm. The red rectangle indicates the time window after the AERONET measurement for which the methodology labelled the aerosol layers (black pixels; aerosol: large-nonspherical) as desert dust.

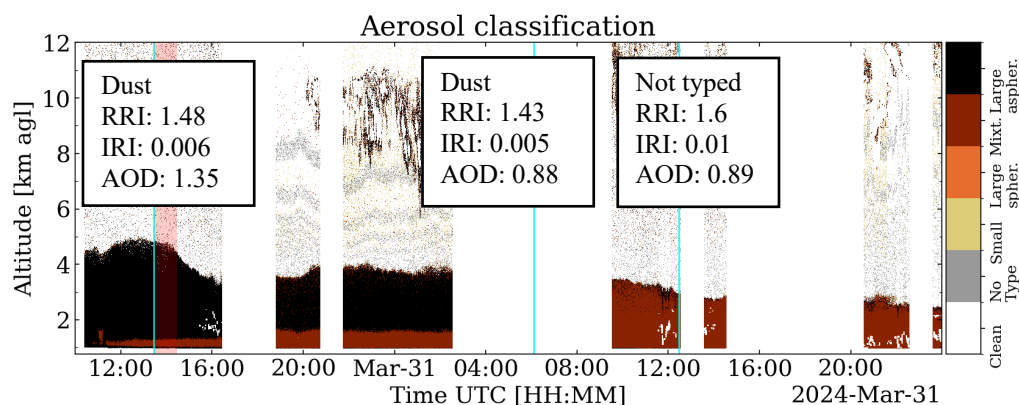


Figure 6: HiRAC aerosol classification retrieved by the CIAO lidar POLPO during 30-31 March 2024. The cyan lines indicate the AERONET measurements for which are given the aerosol type, the complex refractive index at 440 nm, and AOD at 440 nm.

4. DISCUSSION AND OUTLOOK

This document lists the developments regarding the Activity 4.11. A dedicated server (PPS) at CNR-IMAA has been set up to host the aerosol typing modules and the products of the activity. PPS runs in parallel with the SCC and provides additional products based on SCC products, originating either from the SCC database or from the ACTRIS/EARLINET database. Currently, *HiRAC*, *MAC*, and *HETEAC-Flex* modules are available, and these modules output files in NetCDF format as described in Section 2. The modules are written in python and can be found in [GitHub](#) on demand.

The NATALI module (Nicolae et al., 2018; see also D4.11.1) is not yet available and needs to be adjusted to be run in PPS. This typing scheme uses a graphical user interface for the retrieval of the output and makes it impossible to run in an automatic way. We plan to untangle the module from the GUI and deploy the module in PPS around B16. Moreover, we will explore the possibility of incorporating the aerosol typing described in del Águila et al. (2025) before the end of the lifetime of ITINERIS.

The developed server infrastructure and the modified modules to adapt to the ACTRIS/EARLINET database is an added value for ITINERIS to provide multiple and homogeneous aerosol typing products. ITINERIS and projects beyond are expected to benefit from the developments of the Activity 4.11. In this regard, EarthCARE's aerosol classification validation with ACTRIS/EARLINET data is expected to make use of this workflow. Furthermore, additional modules and products are developed within PPS, such as the early warning for aviation algorithm (EWA; Papagiannopoulos et al., 2020), and pollen-specific products for the project SYLVA (A System for Real Time Observation of Aeroallergens; <https://sylvia.bioaerosol.eu/>).

REFERENCES

- Ansmann et al., Ash and fine-mode particle mass profiles from EARLINET-AERONET observations over central Europe after the eruptions of the Eyjafjallajökull volcano in 2010, *J. Geophys. Res.*, 116, D00U02, doi:10.1029/2010JD015567, 2011.
- Baars et al., Target categorization of aerosol and clouds by continuous multiwavelength-polarization lidar measurements, *Atmos. Meas. Tech.*, 10, 3175–3201, <https://doi.org/10.5194/amt-10-3175-2017>, 2017.
- Dawson et al., Spaceborne observations of the lidar ratio of marine aerosols, *Atmos. Chem. Phys.*, 15, 3241–3255, <https://doi.org/10.5194/acp-15-3241-2015>, 2015.
- del Águila et al., Aerosol type classification with machine learning techniques applied to multiwavelength lidar data from EARLINET, *EGUsphere* [preprint], <https://doi.org/10.5194/egusphere-2025-269>, 2025.
- Floutsi et al., HETEAC-Flex: an optimal estimation method for aerosol typing based on lidar-derived intensive optical properties, *Atmos. Meas. Tech.*, 17, 693–714, <https://doi.org/10.5194/amt-17-693-2024>, 2024.
- Mortier et al., Detection and characterization of volcanic ash plumes over Lille during the Eyjafjallajökull eruption, *Atmos. Chem. Phys.*, 13, 3705–3720, <https://doi.org/10.5194/acp-13-3705-2013>, 2013.
- Nicolae et al., *Atmos. Chem. Phys.*, 18, 14511–14537, <https://doi.org/10.5194/acp-18-14511-2018>, 2018.
- Papagiannopoulos et al., An automatic observation-based aerosol typing method for EARLINET, *Atmos. Chem. Phys.*, 18, 15879–15901, <https://doi.org/10.5194/acp-18-15879-2018>, 2018.
- Papagiannopoulos et al., An EARLINET early warning system for atmospheric aerosol aviation hazards, *Atmos. Chem. Phys.*, 20, 10775–10789, <https://doi.org/10.5194/acp-20-10775-2020>, 2020.
- Wandinger et al., HETEAC – the Hybrid End-To-End Aerosol Classification model for EarthCARE, *Atmos. Meas. Tech.*, 16, 2485–2510, <https://doi.org/10.5194/amt-16-2485-2023>, 2023.
- Weinzierl et al., On the visibility of airborne volcanic ash and mineral dust from the pilot’s perspective in flight, *Phys. Chem. Earth*, 45–46, 87–102, doi:10.1016/j.pce.2012.04.003, 2012.